49 pages

STRUCTURAL CHARACTERIZATION AND GAS REACTIONS OF SMALL METAL PARTICLES BY HIGH-RESOLUTION TEM AND TED

Semi-Annual Technical Report

for the Period
January 1, 1985 to June 30, 1985

Submitted to

National Aeronautics and Space Administration
Ames Research Center
Moffett Field, CA 94305

Computational Chemistry and Aerodynamics Branch
Dr. Jim Arnold, Chief
Dr. Helmut Poppa, Technical Monitor

Grant No.
NCC 2-283

Prepared by

ELORET INSTITUTE
1178 Maraschino Drive
Sunnyvale, CA 94087
(Phone: (408) 730-8422)
K. Heinemann, President and Principal Investigator

STRUCTURAL CHARACTERIZATION AND GAS REACTIONS OF SMALL METAL PARTICLES BY HIGH-RESOLUTION TEM AND TED

by Klaus Heinemann

ELORET INSTITUTE, 1178 Maraschino Drive, Sunnyvale CA 94087
Work performed at NASA-Ames Research Center, Moffett Field, CA 94035

ABSTRACT

The interaction of 100 and 200 keV electron beams with amorphous alumina, titania, and aluminum nitride substrates and nanometer-size palladium particulate deposits was investigated for the two extreme cases of (a) large-area electron-beam flash-heating and (b) small-area high-intensity electron-beam irradiation. The former simulates a short-term heating effect with minimum electron irradiation exposure, the latter simulates high-dosage irradiation with minimum heating effect. All alumina and titania samples responded to the flash-heating treatment with significant recrystallization. However, the size, crystal structure, shape, and orientation of the grains depended on the type and thickness of the films and the thickness of the Pd deposit. High-dosage electron irradiation also readily crystallized the alumina substrate films but did not affect the titania films. The alumina recrystallization products were usually either all in the alpha phase, or they were a mixture of small grains in a number of low-temperature phases including $\gamma, \delta, \chi, \beta, \theta$-alumina. Palladium deposits reacted heavily with the alumina substrates during either treatment, but they were very little affected when supported on titania. Both treatments had the same, less prominent localized crystallization effect on aluminum nitride films.

INTRODUCTION

The transmission electron microscope (TEM) has become a powerful tool in the study of nanometer-size supported metal particles (1), including model structure-sensitive supported catalyst systems (2). It has been established that the catalytic properties of certain structure-sensitive catalysts increase rapidly with deminishing particle size. For example, the rate of CO decomposition of Pd particles supported on muscovite mica increases five-fold when reducing the particle size from 5 nm, at which size the catalytic activity is close to that of bulk Pd, to 2 nm (3). A similar size dependence was found for Ni/mica (4) and Ru/mica (5). It is, therefore, of interest to be able to image particles at highest possible resolution.

It has long been known that the electron beam can have a marked effect on the imaged subject matter, and efforts to reduce the specimen exposure, such as by using an image intensifier system (6) or by optimally taking advantage of the electron speed and fine grain size of TEM photomaterial, have been standard practice. However, the increased availability of very high resolution microscopes that allow, for instance, observation of crystal lattice planes at 1 million times electron optical magnification directly on the microscope fluorescent screen, has increased the "standard" specimen

exposure to such high levels that electron irradiation damage has become a serious problem even for specimens that, when examined at some 100,000 times magnification, could be considered resistant to electron exposure damage. Typical electron current densities at the illuminated specimen area are in the 1-10 A/cm2 for such high-magnification work, compared to 0.001 to 0.01 A/cm2 when working at 100,000 X magnification under conscienciously low irradiation conditions -- whereby such magnifications can still lead to 0.4 nm specimen resolution if reasonably fine-grain photomaterial (e.g., Kodak Electron Image Plates or Electron Image Film #4463) and appropriately high light-optical magnification of the micrographs is used. Aluminum oxide support films have, for example, been considered safe in terms of radiation damage under such conservative mA/cm2 range operating conditions.

This paper describes observations with such films as well as titania and aluminum nitride films under 1-10 A/cm2 operating conditions, where not only rate- and dosage- dependent radiation damage, but also local specimen heating must be considered as possible effect of the primary electron beam. An attempt is made to differenciate between the thermal and the "genuine" radiation damage (breaking of chemical bonds; displacement damage). Alumina and titania films were used because of the significance of these oxide supports in catalysis and, in the case of alumina, a substantial prior TEM work with these films in our laboratory (7-10). The films are examined with and without a particulate deposit of palladium, in order to include e-beam induced metal/substrate interactions in the study. Palladium was chosen because of the number of previous and

current research projects conducted at the NASA-Ames research laboratory and other places (e.g., 1,2,3,11-13). In addition to aluminum nitride, which we are using as an example for a highly current density-sensitive film, we are comparing our results with muscovite mica films, which have also extensively been used in our laboratory (3-5,15) and which are known to suffer chemical bond-breaking and displacement-type radiation damage (16). Although it is known that the degree of radiation damage induced in a TEM specimen depends on the microscope operating voltage, we are indiscriminately using 100 and 200 keV in conformance with the design beam energy of the two microscopes employed in this study, but we are confident that the generality of our conclusions is not affected by this discrepancy.

EXPERIMENTAL

Amorphous alumina films were prepared by anodic oxidation of aluminum foil and by reactive sputter deposition. Two different film thicknesses of anodic films were used, approximately 35 nm and 60 nm. In both cases, the films were stretched over 200-mesh copper grids after dissolution of the supporting aluminum foil in a mercury chloride solution and repeated washing of the remaining alumina film with destilled water. Amorphous titania and aluminum nitride films were prepared by reactive sputter deposition. All sputter deposited films were supported on an "ultrathin" carbon film (less than 10 nm thick) stretched over 200-mesh copper grids.

Palladium was deposited on ex-situ prepared alumina and titania

films from a wire source under 10^{-9} mbar vacuum conditions. Immediately prior to the depositions, the substrates were oxygen plasma treated for cleaning and providing complete stoicheometry of the substrate surfaces. Two different deposit thicknesses were used. The "thin" deposits are characterized by islands of some 1.5-2 nm mean diameter, the "thick" deposits had island sizes in the 3-4 nm size range and were past the initial stage of growth coalescence. In all cases, the particle number densities ranged between $3*10^{12}$ and $8*10^{12}$ cm^{-1}.

The as-received, undeposited films and the Pd-deposited films were examined in high-resolution transmission electron microscopes and subjected to flash-electron treatments and high-intensity electron exposure treatments. An electron current density of 3.6 A/cm2 was typically used for both treatments. The flash-electron treatments were performed in a Hitachi H500H TEM at 100 keV accelerating voltage, the exposure treatments were mostly performed with a Jeol 2000EX instrument at 200 kV.

The flash-electron treatment was designed to simulate a short-term heating effect on the specimen, while subjecting the treated specimen area to only little radiation damage. The treatment duration was typically of the order of 0.1 seconds, achieved by quickly changing the illumination through focus with the final TEM condenser lens. In the focussed condition, the beam diameter was about 30 μm on the specimen (low excitation of first condenser lens). At 3.6 A/cm2 current density, this gives a total specimen current of $2.5*10^{-5}$ A (affecting significant local specimen heating), while the total irradiation dose was below 1 Asec/cm2.

The high-intensity electron exposure treatment was designed to simulate significant electron irradiation while only little affecting the local substrate temperatures. Typical exposure treatments lasted several minutes and were confined to 500 nm specimen areas. The high irradiation intensities of 3.6 A/cm2 could be achieved with a LaB6 filament using a standard condenser 2 aperture in the JEM 2000EX instrument. (They represent, in fact, the standard high magnification operating conditions with this microscope -- required for 1-second exposure times of standard photo material at 600,000X magnification; for observing crystallographic lattice planes on the screen, one often exceeds this magnification while maintaining image current densities in the low 10^{-11} A/cm2 range, thus further increasing the current density in the specimen). At a typical exposure period of 5 minutes, the total irradiation dose computes to some 1000 Asec/cm2, which is over 1000 times the dose experienced during flash electron treatment, while the total current, which is a measure of the temperature rise of the irradiated area, is only $7*10^{-9}$ A, or less than 1/1000 of the current prevailing during flash treatment.

RESULTS

The flash electron treatment instantaneously recrystallized all films, with and without deposit. Whereas for the case of titania the crystallization product was always the same, with the possible exception of bare titania films that crystallized not only to TiO2 grains but showed evidence of some monoclinic Ti3O5 grains as well, the type of alumina crystallization products depended on film thickness, type of film (anodic or sputter-deposited), and on the thickness of the Pd deposit. The high-intensity electron-beam exposure treatment had a very marked effect on the alumina films and Pd particles supported on alumina substrates, while titania films were not affected by this treatment, and Pd particles supported on titania films only suffered a minor degree of coalescence. The findings are summarized in table 1 and described in detail in the following subsections.

(1) Alumina substrates, flash-electron treatment

All anodically prepared bare alumina films crystallized to alpha-Al2O3. The ease of performing this crystallization increased with increasing film thickness. Above some 40 nm in film thickness, the crystallized film areas tended to be stabile and consisted of large grains (up to several tens of square micrometers in area) of alpha-alumina in various orientations, as was shown in earlier work by Heinemann et al (7). The central alpha region is surrounded by a polycrystalline (gamma and delta alumina) zone which borders on the

original, amorphous alumina film. Thinner films would tend to rupture during the flash-electron treatment, and the recrystallized lamellae tended to succumb to the surface tension and ended up forming droplet-like crystals.

The sputter-deposited alumina films, which were 20 nm thick and supported on ultrathin carbon, responded to the flash-electron treatment by crystallizing to much finer-grain films composed of mostly delta-alumina. As Fig.1 shows as typical example, the grain size averages about 30-50 nm, and many voids are found at the grain boundaries, probably pinning the grains during growth. Diffraction analysis suggests the existence of some gamma alumina grains, and possibly also other low-temperature alumina phases, side by side with a majority of delta grains. It should be noted that electron diffraction patterns of aluminas in various phases, except for Boehmite, alpha- and chi-alumina, have so many commonalities that it is often very difficult or impossible to clearly differentiate between them on the basis of the experimental evidence provided by high-resolution TEM and TED of small selected areas. We do, however, at times venture to express a preference if the results so justify.

The behavior of Pd-deposited alumina films was studied for the case of thick anodically prepared support films that would without deposit easily recrystallize to the alpha phase upon flash heating. Thin palladium deposits, i.e., particles of 1-2 nm size and some $5*10^{12}$ cm^{-2} number density, would not alter this substrate recrystallization behavior. However, when the deposit was thicker, the substrate would crystallize to much smaller crystals of some 50 nm mean size. Fig.2 illustrates what happens both to the substrate

and the deposit in this case. Approaching from left to right in 5 micrometer increments the center of the recrystallized area (see top part of Fig.2 as partial overview), we observe the following details: Still quite distant from the center of the recrystallized area, the Pd deposit exhibits substantial coalescence (Fig.2b), and voids begin to form in the substrate, while the film is still amorphous (see diffraction pattern to Fig.2b; this pattern is virtually identical to that of Fig.2a which is therefore not shown). At the next stage (Fig.2c), substrate crystallization has started, the deposit particles have coalesced to what can be recognized as the mean substrate crystal size, and the voids have coalesced to the 5 nm size range. Progressing further toward the center, many of the voids join and mark the boundaries of the alumina grains, while the Pd particles seem to have disappeared. The diffraction patterns in Fig.2 reveal, with due caution, that the main phase of alumina generated during flash heating is kappa-Al2O3.

The void network is substantiated with Fig.3 which shows the center of the recrystallized Pd-deposited film in strong underfocus (a), near Gaussian focus (b), and in strong overfocus (c), evidencing contrast reversal as is typical for voids. Further visible in Fig.3, and more clearly demonstrated at higher magnification (Fig.4), are interference fringes reaching across whole grains. The spacings of these fringes suggest that they are moires between Pd(111) and Pd(220) planes and most likely kappa-Al2O3 crystal planes. The same types of moire fringes were found in the polycrystalline zone of flash-electron treated alumina films that carried only a thin Pd deposit. Fig.5 depicts in (a) an area within the alpha-zone, where no

moires were found, in (b) a polycrystalline region exhibiting 7 nm moire fringes, and in (c) an area within the amorphous substrate that had still been hot enough during the flash heating process to induce major coalescence of the Pd deposit particles. (Fig.9a shows the original Pd deposit of this sample).

(2) Alumina substrates, high-intensity electron exposure

Irradiation with electron beams at intensities exceeding 2 A/cm2 crystallized all our alumina film samples and strongly affected the appearance of the Pd deposits, but the specifics of the e-beam exposure-induced changes depended on the type of alumina film and the thickness of the deposit. Irradiation of up to 4 minutes at 1 A/cm2 and as much as 90 min at 0.01 A/cm2 did, however, not induce any changes in any of the bare and Pd-deposited alumina films. Only very long-term exposure, such as 10 hrs at 0.01 A/cm2, would eventually induce measurable substrate crystallization (17).

When applying our standard irradiation condition of 3.6 A/cm2 to the thin anodically prepared bare alumina film samples, changes became apparent after about one minute. Fig.6 shows wide-spread recrystallization to grains of varying small size (most less than 10 nm), obtained after 8 minutes of irradiation. The grains are still surrounded by amorphous alumina, but the boundaries are well defined, although not marked by voids. Lattice spacings of 2.0nm, 2.4nm, 2.8nm, and 4.6nm were measured in high-resolution micrographs of these samples (Fig.6 contains all these spacings). They can be attributed to gamma and possibly other low-temperature alumina phases (kappa, beta, theta, delta) of alumina, with gamma providing the most probable fit when considering the selected area diffraction results (Fig.6b) and the light optical diffraction results (Fig.6c) taken from the same area imaged in Fig.6a. This diffractogram indicates that spacings other than 0.1977 nm and 0.28 nm (the 400 and 220 planes of gamma alumina, respectively), that clearly do occur occasionally as can be seen in Fig.6a, range over very small areas

and in random orientations, such that in mean intensity they only contribute to a diffuse center zone in the diffractogram. No alpha-alumina was found in any of our high-intensity esposure treated samples. Further irradiation, including at higher current densities (our facilities allowed to go up to 6 A/cm2 while maintain the lattice plane resolution capability) did enhance the degree of recrystallization but did not change the recrystallization product.

The only differences to these observations when going to thicker anodic alumina films are that in this case we occasionally also find grains with 4.6nm, 2.8nm, and 2.4nm cross lattice fringes at intersecting angles that positively identify cubic gamma-Al2O3 crystals, as is demonstrated in Fig.7, and that after only 3 minutes of irradiation the entire irradiated area is recrystallized, leaving no amorphous alumina surrounding the grains.

Electron exposure treated sputter-deposited alumina show the (220), (111), and (311) cross lattices of gamma Al2O3 even more pronounced than thick anodic films, and the grain boundaries are undefined. An example is shown in Fig.8.

When the electron-irradiated alumina substrate films carry palladium particles, the following observations were made for high-intensity electron exposure: First, the substrate film is recrystallized to predominantly gamma alumina, very similar to an undeposited film. Second, the grain boundaries are now clearly marked, as can be seen in Fig.9a, which was taken after a 2-min exposure to an electron beam of 3.6 A/cm2 intensity, and in Fig.9b-d, which depict the same area after 12 minutes total exposure. Third, the palladium particles, still present after 2 minutes exposure

(Fig.9a), have enormously coalesced (compare particles in center feature in Fig.9a and 9b) or, in most areas, completely disappeared after the longer exposure. In contrast to the changes observed for these samples after flash-electron treatment, we did in this case not find moire fringes that would evidence spreading of the palladium over the substrate crystals. On the other hand, a large number of checked areas of some 3-5 nm in diameter was noted. These features, which are particularly well visible in particle A in Fig.9c, were not observed in electron irradiated bare alumina films and could well be due to, or remnants of, the original palladium deposit particles. This conclusion is corroborated by the observation that they decrease in size and contrast when subjecting an alumina films with a thinner Pd deposit (smaller particles at same number density) to the same irradiation treatment.

(3) Titania substrates, flash-electron treatment

Recrystallization of amorphous titania films by electron flash-heating occurred easily and required less beam intensity than alumina films. A typical example is given in Fig.10 which shows in (a) at low magnification a section of a recrystallized area of approximately 30 micrometer diameter, and in (b) at high magnification a portion of two adjacent TiO2 grains, with the corresponding light optical diffractogram as insert. The 0.69 nm fringes are tentatively interpreted as surface-reconstructed 101 planes of the tetragonal crystal. They are uniform in direction and contrast over large areas and indicate low-defect densities in the titania crystals. The carbon support film underneath the crystals is visible by the phase contrast features in the background of Fig.10b. Some crystals in the outer zone near the not crystallized titania film, such as shown in Fig.11, show a cross lattice with .35nm and .47nm fringes and are tentatively identified as Ti3O5 crystals.

Recrystallization to TiO2 of Pd-deposited amorphous titania films upon flash-electron treatment occurs virtually identically to bare titania films. In contrast to Pd/alumina, the only notable change to the Pd deposit is a minor degree of coalescence, as is shown in Fig.12, where (a) is the Pd/TiO2 film as-transferred to the TEM, (b) is the crystalline/ amorphous border region (A & B are portions of two crystals, C is amorphous titania), and (c) is the center of the flash-electron treated area. Even less coalescence was noted for heavier Pd-deposited films.

(4) Titania substrates, high-intensity electron exposure

Exposure of titania films to electron beams at current densities of 3.6 A/cm2 had no effect that could be quantified by high-resolution TEM and TED. The only exception is some coalescence of a thin Pd deposit. This is shown in Fig.13, where (a) shows the untreated film, (b) the same general area after 30-sec beam exposure, and (c) the same area after 5-min beam exposure. In particular, no effect was noted for bare amorphous films and bare recrystallized films -- images such as shown in Fig.10 were reproduced after tens of minutes of high-intensity irradiation. The coalescence effect noted with Fig.13 was not observed when the current density was lowered to 2 A/cm2.

(5) Aluminum nitride substrates

20 nm thick AlN films, supported on ultrathin carbon, would not recrystallize under electron flash treatment conditions in any way similar to alumina and titania films. However, e-beam flash heating does induce in AlN films crystallization to very small grains of some 5 nm mean size, embedded in the amorphous nitride film and with very poorly defined grain boundaries. The same recrystallization result was found upon high-intensity irradiation. Fig.14 shows an example of a bare AlN film treated for 5 min with an electron beam of 3.6 A/cm2 intensity. The lattice spacing of 0.27 nm measured in many grains in the image can be attributed to 100 planes of hexagonal AlN, and the electron diffraction patterns confirm this crystal structure. Crystallization of AlN films occurred, very unlike alumina and titania films, already at very low irradiation dosages. Within one minute of irradiating at only 0.15 A/cm2, the originally uniformly amorphous film had already changed to the appearance shown in Fig.14.

DISCUSSION

The recrystallization effect using large-area electron-beam flash-heating has been extensively used in our laboratory for the case of alumina (7 – 10) and was first demonstrated by Francombe et al (18) for various metal oxides such as titania, zirconia, tantala, and alumina. Virtually identical e-beam heating conditions were also previously used to "cleave" MgO crystals in-situ into electron-beam transparent film areas (11, 12, 13, 20). The subject of temperature increase of the flash-exposed area was discussed in a rudimentary form in one of these papers (11) on the basis of original work by Castaign (21) who related the temperature increase, ΔT, in the center of the irradiated area with the relevant experimental parameters as follows:

$$\Delta T = \frac{V I_0 \sigma}{4\pi\alpha C}\left(1 + 2\ln\left(\frac{b}{a}\right)\right) \qquad \text{(equ.1)}$$

In this equation, I_0 and 2b are the total specimen current and the diameter of the illuminated specimen area, respectively. Using an acceleration voltage of 100 kV, I_0 = 25 μA, b=15 μm, and a specimen thickness of a=50 nm, as well as α=4.18 J cal^{-1} as mechanical heat equivalent, C=0.02 cal/(cm sec K) as thermal conductivity of the substrate, and σ=40 cm^{-1} as electron absorption coefficient of the specimen, we get $\Delta T \approx 1180$ K, i.e., a temperature rise well sufficient to recrystallize amorphous alumina to the alpha-phase. On the other hand, if one applies the high-intensity exposure treatment conditions used in our experiments, i.e., I_0=7 nA, b=250 nm, and a=50

nm, we get ΔT=0.11 K, which is truly an insignificant temperature rise and, therefore, fully justifies the consideration of these two cases as exclusively thermal (flash-heating) or irradiation (high-intensity exposure) treatments, respectively. The observation of quite different results for these two treatments, such as was found for titania films, is therefore expected, whereas the observation of quite similar, strong effects for both treatments for the cases of alumina and aluminum nitride films is, in fact, at first glance unexpected. The former characterizes for all practical purposes insensitivity towards electron irradiation damage, the latter describes some degree of irradiation damage sensitivity.

The observation that the crystallization product of alumina films with and without deposit upon flash electron treatment varies with type and thickness of film and deposit is consistent with equ.1 which suggests a decrease of ΔT when the thermal conductivity of the film increases, such as by an underlying carbon support film or a layer-type metal deposit. The former explains why the sputter-deposited alumina films, which were supported by thin carbon films, recrystallized to a lower-temperature alumina phase (see Tab.1), whereas self-supporting anodic alumina films recrystallized to the alpha-phase; and the latter explains why under otherwise identical conditions a self-supporting anodic alumina film with a thick Pd deposit was found to recrystallize to lower-temperature phases, compared to thin Pd/alumina deposits for which the recrystallization product is the same as for bare alumina films, i.e., alpha-alumina.

The explanation of a layer-type metal deposit reducing the film

temperature during e-beam flash-heating also corroborates the unexpected finding, suggested by the Pd/alumina moires (Fig.4), that the palladium particles do not evaporate during the flash-heating treatment, as one might expect from a phenomenological extrapolation of the coalescence behavior noted with Fig.2 (three left micrographs), but that the strongly coalesced particles eventually collapse and spread as thin, continuous films over entire grains of the substrate. This spreading process must then have occurred at a temperature well below 1500 K, at which the alpha-phase forms, but quite likely above 1200 K, at which the kappa-phase forms (22) which was identified as most likely predominant crystallization product for alumina films with thick Pd deposits. This high conversion temperature may be the explanation why spreading of Pd over alumina crystal surfaces had not been detected in earlier work such as the Pd/alumina model studies recently reported by Baker et al. (2) where 800 C was the upper temperature limit investigated.

We have in earlier in-situ TEM studies on recrystallized alumina substrates emphasized the re-evaporation of thin metal deposits during a renewed e-beam flash-heating recrystallization process as a major advantage of such in-situ studies in that one specimen could in principle be used over and over by generating a clean substrate after each crystallization (10). This statement may well apply to certain deposit materials including Si (10), Fe (9), and Au (11), for which we did not find any evidence of deposit/substrate moires, and in which case renewed e-beam flash heating lead to crystallization to the alpha phase, with no apparent difference to the crystalization mechanism of bare alumina films; but the example of Pd/alumnia

certainly does demonstrate that generalization of the statement is in error. Due to the metal film spreading upon flash heating, in-situ studies with catalytically active systems, such as Pd/alumina and possibly Pt and other metals on alumina, require a new substrate film for each in-situ deposition /reaction experiment (14).

The observation of voids in all flash-electron heated alumina crystallization products (see also (7) for th case of alpha-alumina) can be rationalized as clustering of vacancies while the time available for these clusters/voids to segregate to the vacuum interface is too short. No voids were found in any of the crystallization products of the high-intensity e-beam exposed samples where the exposure/annealing times were much longer. It would be interesting to persue if the voids created during flash-heating could be used for in-situ TEM model catalytic studies with micro-porous aluminas. Whereas the voids remaining within the individual recrystallized grains (Fig.3) may be difficult to impregnate with a catalyst, voids at the grain boundaries may lend themselves more readily to impregnation with Pd of Pt catalysts, since at least a larger number of them is presumably open to the vacuum interface. Nevertheless, none of the voids seem to have been filled with Pd during the above described deposit spreading process, as is evidenced by the contrast reversal in Fig.3, except for a few very small particles that can be seen predominantly near voids and have a much smaller size than the voids (see the arrows in Fig.3 as example; these particles have, in fact, not positively been identified as Pd).

The observation of substantial substrate crystallization upon

high-intensity electron exposure of amorphous alumina substrates, with and without Pd deposit, can only be explained as intrinsic electron irradiation sensitivity of amorphous alumina substrates. Whereas amorphous titania is completely insensitive to this irradiation treatment, the observed easy crystallization of amorphous Al2O3 by e-beam exposure may be consequential of the existence of randomly oriented "molecular" units, perhaps $(Al_2O_3)_2$, as was suggested by Wilsdorf (**23**), the e-beam providing the threshhold energy for crystallization to the lower free energy crystalline state.

Most significant is, however, that during this "classical" radiation damage process a palladium deposit is changed beyond recognition when compared to the as-deposited morphological appearance (Fig.9) of the deposit. This drastic change of appearance of small Pd particles is clearly not found on titania substrates (Fig.13) that themselves remain inert to high-intensity electron exposure. However, it was also not observed for Pd/mica deposits where the substrate is known to suffer strong radiation damage (**16**) -- in this case destroying the crystalline order of this Al-Mg-silicate film -- while the Pd particles remain unaffected (Fig.15). Fig.15 shows an example of a thin Pd deposit on mica after 1 min, 3 min, and 7 min irradiation at 3.6 A/cm2 in (a), (b), and (c), respectively. Whereas the mica lattice planes are still visible in (a), they are clearly destroyed in (b) and (c), yet the mica particles (about 1 nm in size) are still clearly visible and seem unchanged. Fig.15d shows an overview of the border region between irradiated (top right) and not irradiated specimen areas. The

Pd/alumina results may indicate a significant, strong interaction between Pd and the alumina substrate under electron irradiation conditions. The interaction may be of a localized thermal rather than a chemical bond-breaking nature, which seems indicated by the circumstance that a crystalline order rather than a disorder, as in the case of mica (Fig.15), results, and by comparing with the e-beam flash-heating results for Pd/alumina deposits where clearly radiation damage, such as Al-O bond destruction by inelastic scattering processes with the primary electrons, can be ruled out as principal reason for the observed effect due to the low irradiation dose in that case. It could be hypothesized that the inelastic scattering events transfer, instead, thermal energy to the individual "bi-alumina" units (23), raising their vibrational frequencies and thus local temperatures to the level that affects localized ordering and spreading of the Pd deposit as was observed for larger-area flash heating. This process would be expected to follow a nucleation and growth process, because, once a crystal nucleus has been formed, the energy required for bi-alumina units to attach to the growing crystal would be lower than the energy required to start a new crystal nucleus. The existence of crystallized islands and, more generally, the observation that the crystallization effect due to high-intensity e-beam exposure is film thickness-dependent and proceeds slower and less prominent for thin amorphous alumina films, where the recrystallized zones were still surrounded with amorphous alumina, was demonstrated with Fig.6, when compared with Fig.7. In this case of a thin alumina film, the possibility of an electron suffering an inelastic scattering event is decreased, and hence a less complete

stage of crystallization was attained in this sample upon "standard" e-beam treatment (of 8 min exposure to 3.6 A/cm2). The observations do, indeed, include complete crystallization of this same sample upon longer and more intense radiation treatment.

As final remark regarding the Pd/alumina interaction upon high-intensity e-beam exposure, one can further conjecture that the large number of checked areas of some 3-5 nm diameter noted in Fig.9b could, in fact, very well be the areas where spreading of the individual original Pd particles on the crystallized substrate ends, possibly due to lack of atoms to form at least one monolayer. (The original particle size in this sample was 1.5 - 2 nm, containing 100 - 200 atoms per particle if spherical particle shape is assumed; if these particles spread out in a monolayer, they would cover an area of some 3-5 nm).

The findings for high-intensity e-beam exposure of titania films with Pd deposit, where some degree of coalescence was found, may at first glance point to a substrate temperature increase. However, this is unlikely for two reasons. First, the simplified theoretical consideration of the actually expected temperature increase would, as was mentioned earlier, contradict any measurable temperature increase under the prevailing small-area illumination conditions. Second, the experimental results show a magnitude of coalescence (Fig.13) quite comparable to the coalescence noted for flash-electron treatment (Fig.12), where it is known that a temperature of some 1000 K is easily reached. We tentatively conjecture that the mechanism may rather have been an e-beam stimulated ripening effect of the particles. This explanation would have to be corroborated with

particle size analyses of micrographs taken before and after high-intensity e-beam exposure (Fig.13a and c, respectively). Such work is in preparation.

The results obtained for AlN films indicate a very strong, dosage-dependent irradiation sensitivity of this material when compared to alumina and titania. Our experiments showed that an irradiation dose of only 1 Asec/cm2, obtained by illuminating for 100 sec at 0.01 A/cm2, will already form small aluminum nitride crystals embedded in the original amorphous film material. This equals the dose applied during typical e-beam flash heating where the film temperature is momentarily raised well above 1000 K, and which condition we justifiedly described as predominantly thermal, with negligible radiation effect, for the case of alumina and titania films.

For reasons of comparison it should be noted that very long-term irradiation at these low current densities of 0.01 A/cm2 would also transform amorphous alumina films to polycrystalline alumina (14,17 This underlines the above suggestion that the radiation sensitivity of alumina is dosage-dependent. The principal difference between alumina and aluminum nitride films, both of which suffer no breakage of chemical bonds as primary radiation effect, then remains the degree of radiation sensitivity, alumina being by a factor of approximately 1000 less sensitive than aluminum nitride.

CONCLUSIONS

The effect of the electron beam in high-performance transmission electron microscopes on various substrates, including alumina, aluminum nitride, and titania films, and on palladium deposits has been investigated. The study has shown that amorphous alumina substrates are much more electron-beam sensitive than titania substrates, and that the electron beam induces a strong reaction between Pd deposit particles and an alumina substrate under irradiation conditions that are typically used for high-resolution TEM imaging. Comparatively little reaction is induced between Pd and titania substrates. Even under shock-thermal treatment conditions, where minimum electron irradiation damage exists, we find a strong Pd/alumina reaction and almost no influence on Pd/titania.

We conclude generally that the electron beam used in TEM , such as for observing supported catalysts, may have a marked influence on the samples under investigation, and that utmost care is advised in the interpretation of the TEM results with regard to intrinsic particle/substrate characteristics and extrinsic electron-beam effects. It would, in fact, seem desirable to generally adopt the practice to report the beam intensity and beam exposure conditions with high-resolution electon micrographs presented in support of scientific findings.

Acknowledgements

The high-resolution TEM work with the JEM 2000EX facility was performed at Xerox Palo Alto Research Laboratories, and we thank in

particular Dr. Fernando Ponce for making this facility available for our use and for stimulating discussions during the course of this work. We also thank Dr. T. Allen of Optical Coatings Laboratories, Inc., in Santa Rosa, California, for providing the sputter-deposited alumina, titania, and aluminum nitride substrate films.

REFERENCES

(1) H. Poppa and K. Heinemann, Optik 56,183, 1980

(2) R.T. Baker, E.B. Prestridge, and G.B. McVicker, J. Catalysis 89, 422, 1984.

(3) D.L. Doering, H. Poppa, and J.T. Dickinson, J. Catalysis 73, 104, 1982.

(4) D.L. Doering, J.T. Dickinson, and H. Poppa, J. Catalysis 73, 91, 1982.

(5) Ch. Park, W.G. Durrer, H. Poppa, and J.T. Dickinson, J. Catalysis, in print.

(6) K. Heinemann and H. Poppa, Proceed. EMSA 1972, p. 610, 612

(7) K. Heinemann, R. Anton, and H. Poppa, Proceed. EMSA 1981, p.158.

(8) R. Anton and K. Heinemann, Proceed. EMSA 1980, p. 402.

(9) R. Anton, H. Poppa, and K. Heinemann, Proceed. EMSA 1981, p.218.

(10) K. Heinemann and T. Osaka, J. Crystal Growth 59, 485, 1982, and H. Poppa, R.D. Moorhead, and K. Heinemann, submitted for publication

(11) K. Heinemann, H.K. Kim, and H. Poppa, J. Vac. Sci. Technol. 16, 622, 1979.

(12) K. Heinemann, T. Osaka, H. Poppa, and M. Avalos-Borja, J. Catalysis 83, 61, 1983.

(13) K. Heinemann, T. Osaka, and H. Poppa, Ultramicroscopy 12, 9, 1983.

(14) K. Heinemann and H. Poppa, in preparation.

(15) K. Heinemann and H. Poppa, Surface Science, in print.

(16) K. Heinemann, Proceed. EMSA 1970, p. 526.

(17) K. Heinemann and H. Poppa, unpublished results.

(18) M.H. Francombe, A.J. Noreika, and S.A. Zeitman, Sect.6, Final Technical Report, Contract AF 33 (615-3814), BPSN - No. 6-684150-415002, 1960.

(19) J.J. Metois, K. Heinemann and H. Poppa, Thin Solid Films 41, 197, 1977.

(20) G. Honjo, S. Shinozaki, and H. Sato, Appl. Phys. Lett. 9, 23, 1966.

(21) R. Castaign, Thesis, Paris 1951.

(22) D.L. Cocke, E.D. Johnson, and R.D. Merrill, Catal. Rev. - Sci. Eng. 26, 163, 1984.

(23) H.G.F. Wilsdorf, Nature 168, 600, 1951.

Table 1 SUMMARY OF RESULTS

Deposit/substrate system	Flash-electron treatment Crystalliz. Product	Remarks	high-intensity e-beam exposure Crystalliz. Product	Remarks
thin anodic Al_2O_3	α-Al_2O_3	(very difficult)	γ-Al_2O_3	(possibly also other low-temp. Al_2O_3 phases)
thick anodic Al_2O_3	α-Al_2O_3	(easy)	γ-Al_2O_3	(some δ-Al_2O_3 grains)
Al_2O_3/C (sputtered)	δ-Al_2O_3	(possibly also $\kappa, \beta, \theta, \gamma$-$Al_2O_3$; voids)	γ-Al_2O_3	(some δ-Al_2O_3 grains; grain boundaries undefined; no voids)
Pd/Al_2O_3 (thin dep.)	α-Al_2O_3	(Pd coalescence; moires; no voids)	γ-Al_2O_3	(Pd particles disappear)
Pd/Al_2O_3 (thick dep.)	κ-Al_2O_3	(possibly also δ, θ, β, and some α-Al_2O_3; moires; voids at grain boundaries; Pd-coalescence)		
TiO_2/C (sputtered)	TiO_2	(possibly some Ti_3O_5)	remains amorphous	
Pd/TiO_2/C (thin dep)	TiO_2	(some coalescence)	remains amorphous; (some Pd-coalescence)	
Pd/TiO_2/C (thick)	TiO_2		remains amorphous (no coalescence at 2 A/cm^2 irradiation)	
AlN (sputtered)	forms small AlN crystals embedded in original amorphous film already at very low electron irradiation dosage (1 Asec/cm^2)			

FIGURE CAPTIONS

Fig.1. Amorphous sputter-deposited 20 nm thick alumina film, supported on carbon, recrystallized by e-beam flash heating.

Fig.2. Palladium on 60 nm thick amorphous, anodically prepared alumina film, e-beam flash heated. From left to right: transition from still amorphous to center of recrystallized substrate region. Top: overview of region between micrographs (c) and (e).

Fig.3. Center of e-beam, flash-heating recrystallized region of Pd/alumina (Fig.2f), in underfocus (a), focus (b), and overfocus (c) to demonstrate voids at grain boundaries and inside of grains by contrast reversal.

Fig.4. Center of e-beam, flash-heating recrystallized region of Pd/alumina (Fig.2f), showing Pd(111) and Pd(220) moire fringes with alumina crystals.

Fig.5. Thin Pd deposit on 60 nm thick amorphous, anodically grown alumina film, recrystallized by e-beam flash heating; center of recrystallized area (a), polycrystalline region (b), and amorphous region near recrystallized area (c).

Fig.6. 40 nm thick amorphous, anodically oxidized alumina film after 8-min e-beam irradiation at 3.6 A/cm2. Diffractogram (lower right) evidences 400 spacing of gamma alumina.

Fig.7. 60 nm thick amorphous, anodically oxidized alumina film after 3-min e-beam irradiation at 3.6 A/cm2. Lattice planes indicate by spacing and direction the gamma alumina crystal.

Fig.8. 20 nm thick sputter-deposited, carbon-supported amorphous alumina film after 10-min e-beam irradiation at 3.6 A/cm2, leading to gamma alumina crystals.

Fig.9. Thin Pd deposit on 60 nm thick amorphous, anodically oxidized alumina film, after 2-min e-beam exposure at 3.6 A/cm2 (a) and after 10 more minutes exposure (b-d); (c) and (d) show higher magnifications of the areas outlined in (b) and (c), respectively.

Fig.10. Sputter-deposited amorphous titania film, supported on carbon film, recrystallized by e-beam flash-heating. Below: center region of recrystallized area, showing grain boundary at top left.

Fig.11. Amorphous/crystalline border region of e-beam, flash-heating recrystallized titania film. Imaged lattice planes suggest Ti_3O_5 crystal.

Fig.12. Amorphous titania film with heavy Pd deposit; as-deposited (a) and recrystallized by e-beam flash heating (b,c). Crystalline/amorphous border region is shown in (b), center of recrystallized region in (c).

Fig.13. Amorphous titania film with heavy Pd deposit; as-deposited (a), and after 30-sec (b) and 300-sec (c) irradiation at 3.6 a/cm2.

Fig.14. Amorphous AlN film, partially crystallized by 5-min irradiation at 3.4 A/cm2.

Fig.15. Thin deposit of Pd on mica, after 1 min (a), 3 min (b), and 7 min (c) irradiation at 3.6 A/cm2; in (d) an overview of the boundary region between irradiated (top right) and not irradiated areas is shown.

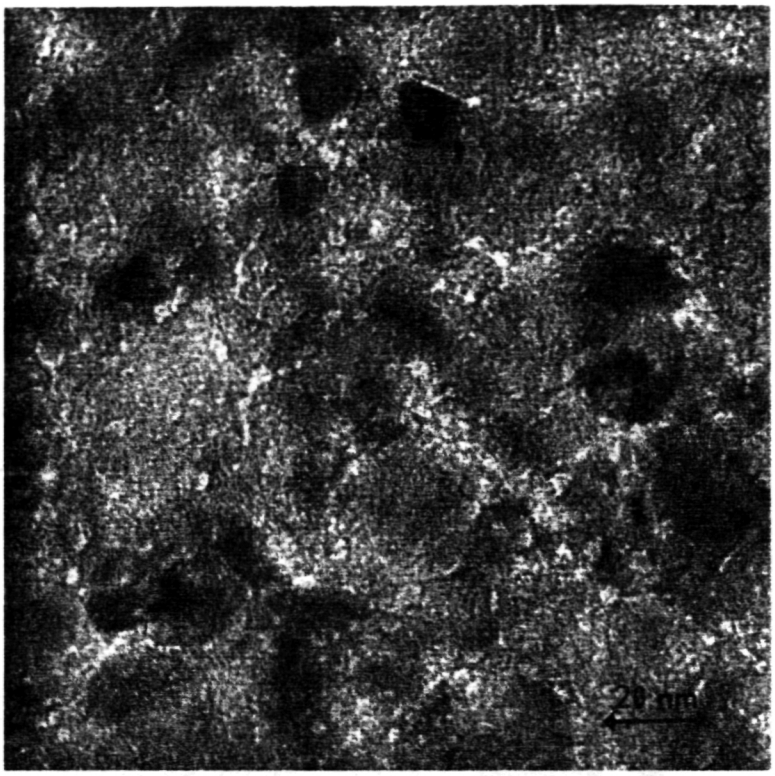

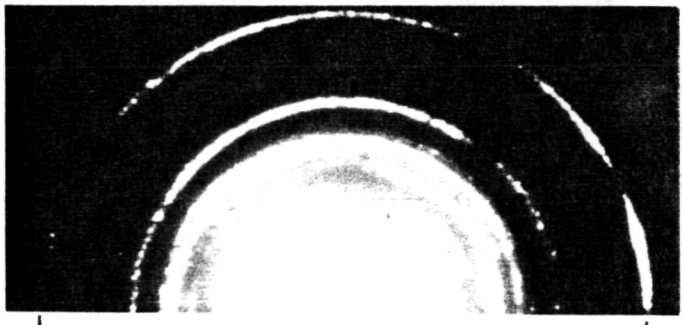

Fig. 1

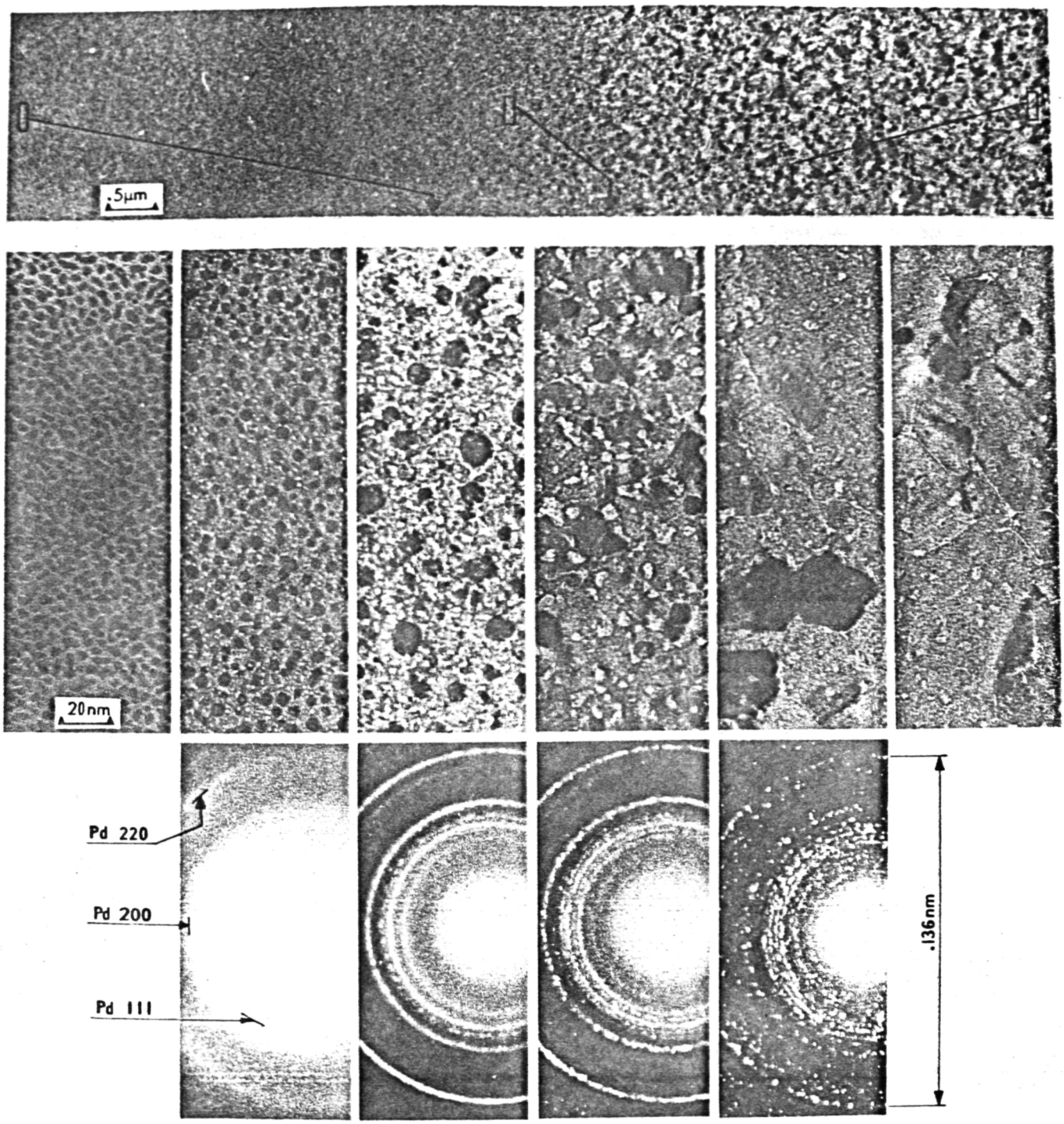

Fig. 2

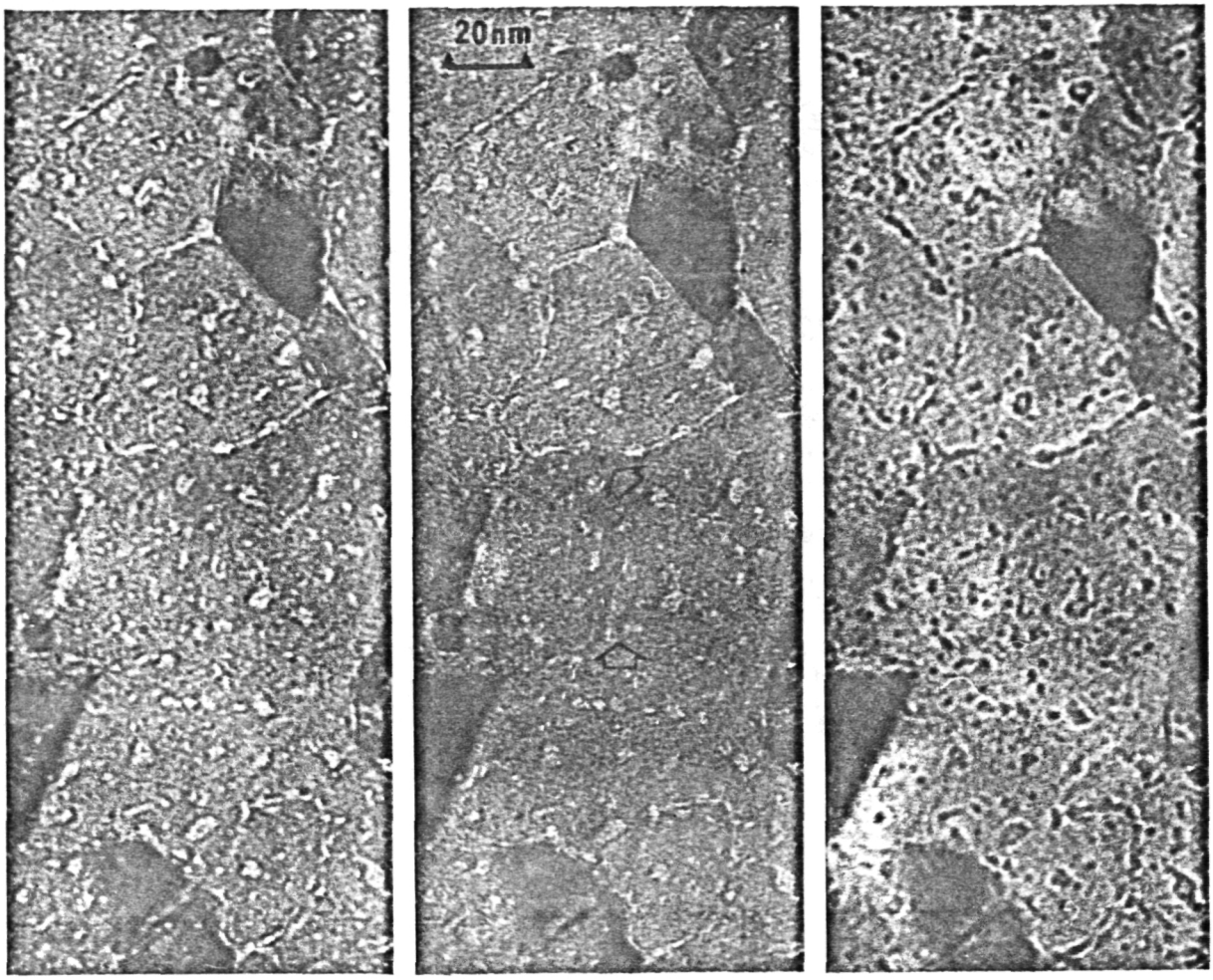

Fig. 3

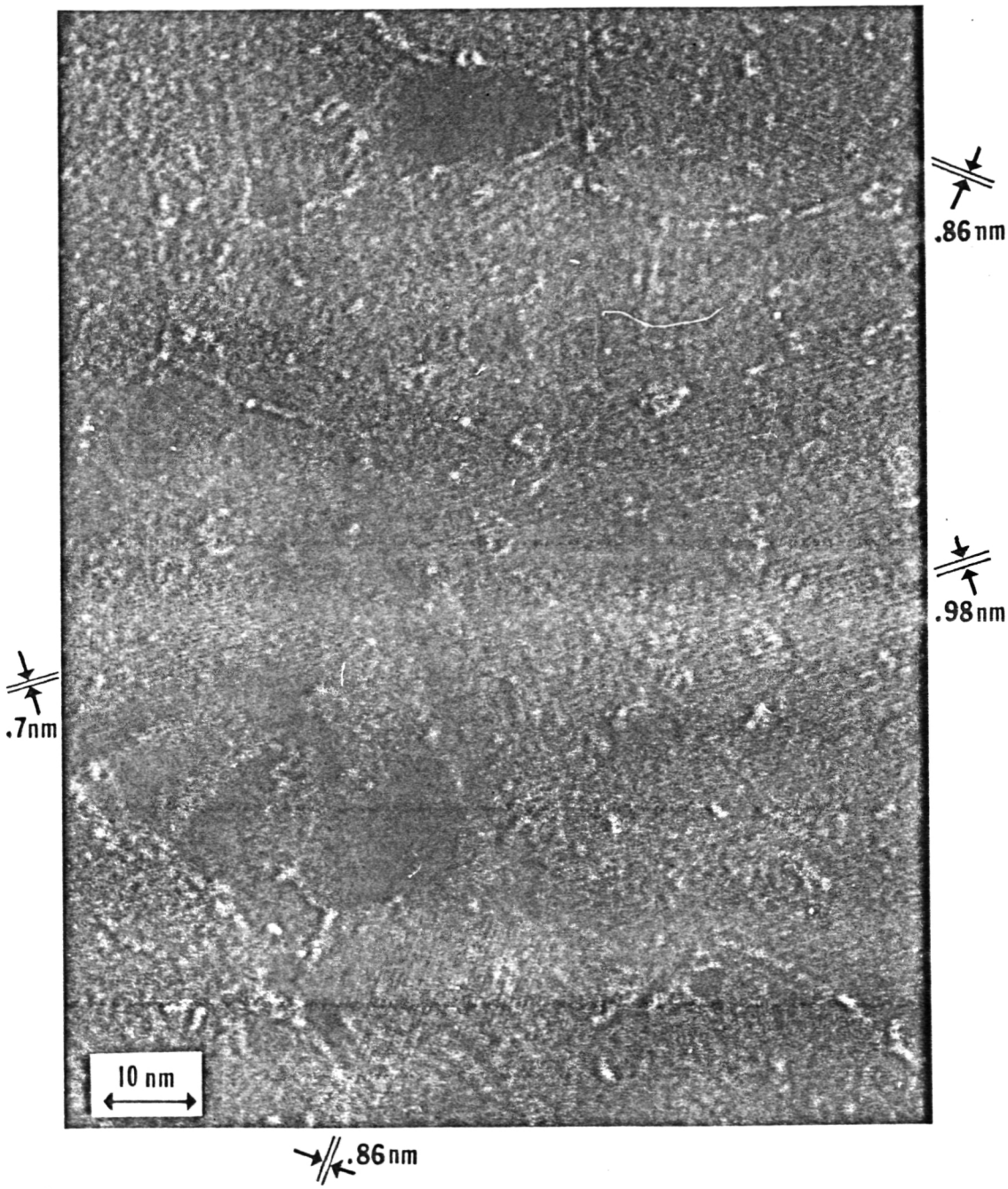

Fig.4

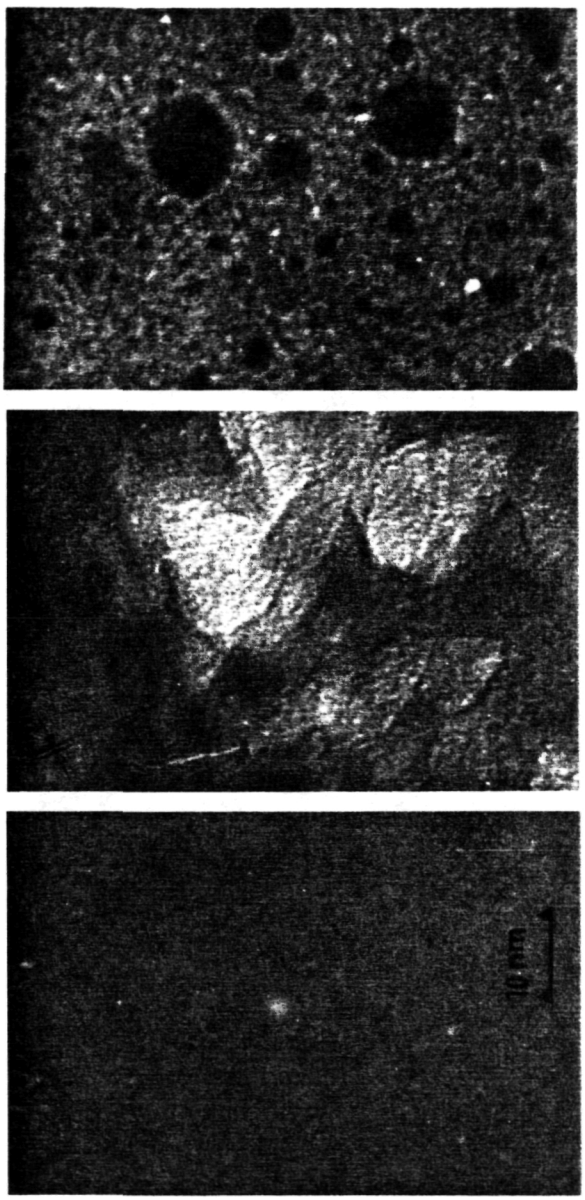

Fig. 5

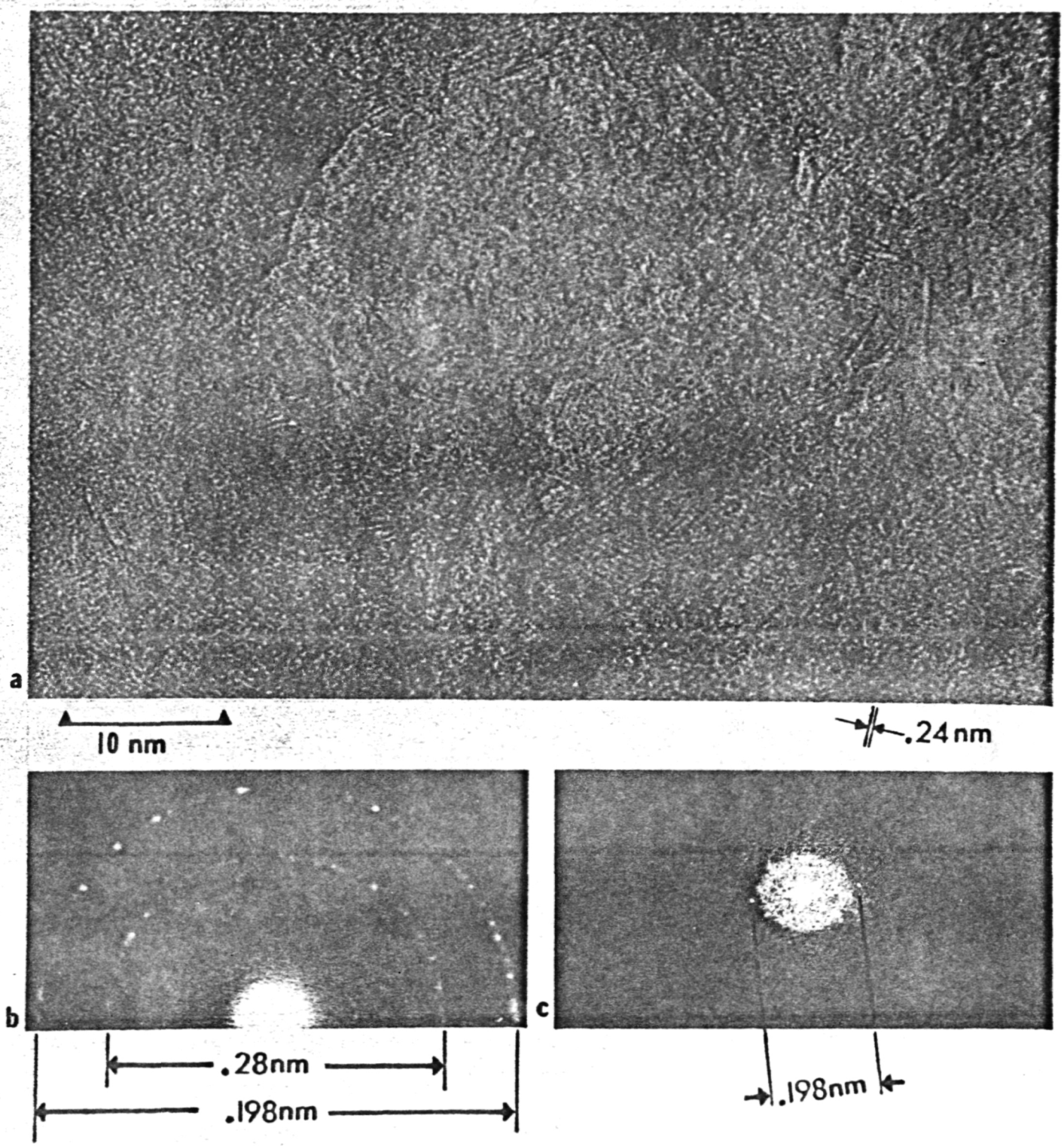

Fig. 6

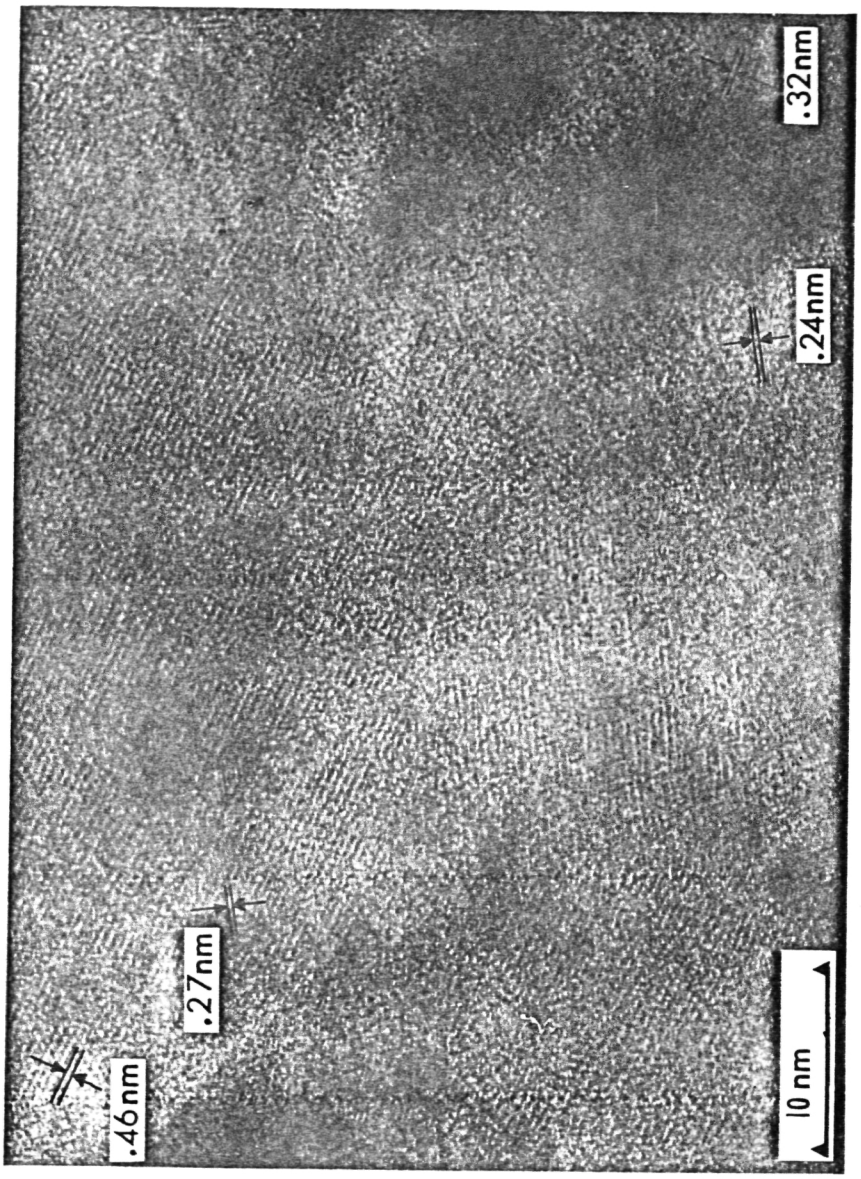

Fig. 7

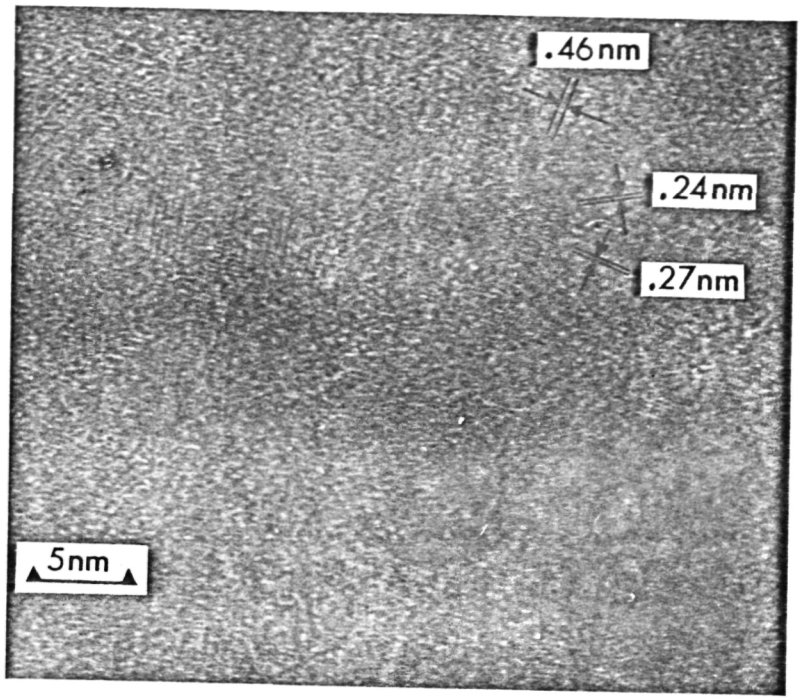

Fig. 8

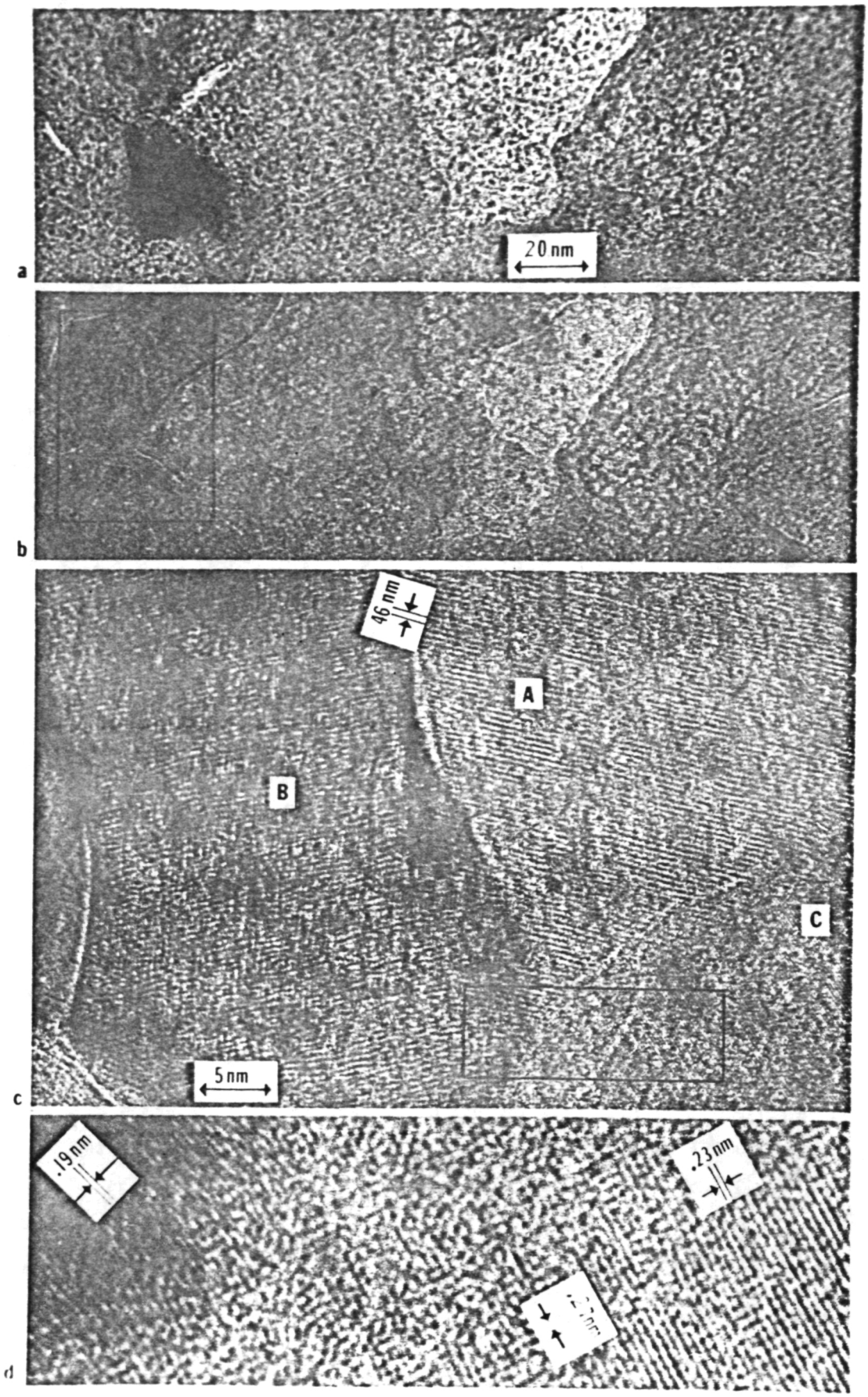

Fig. 9

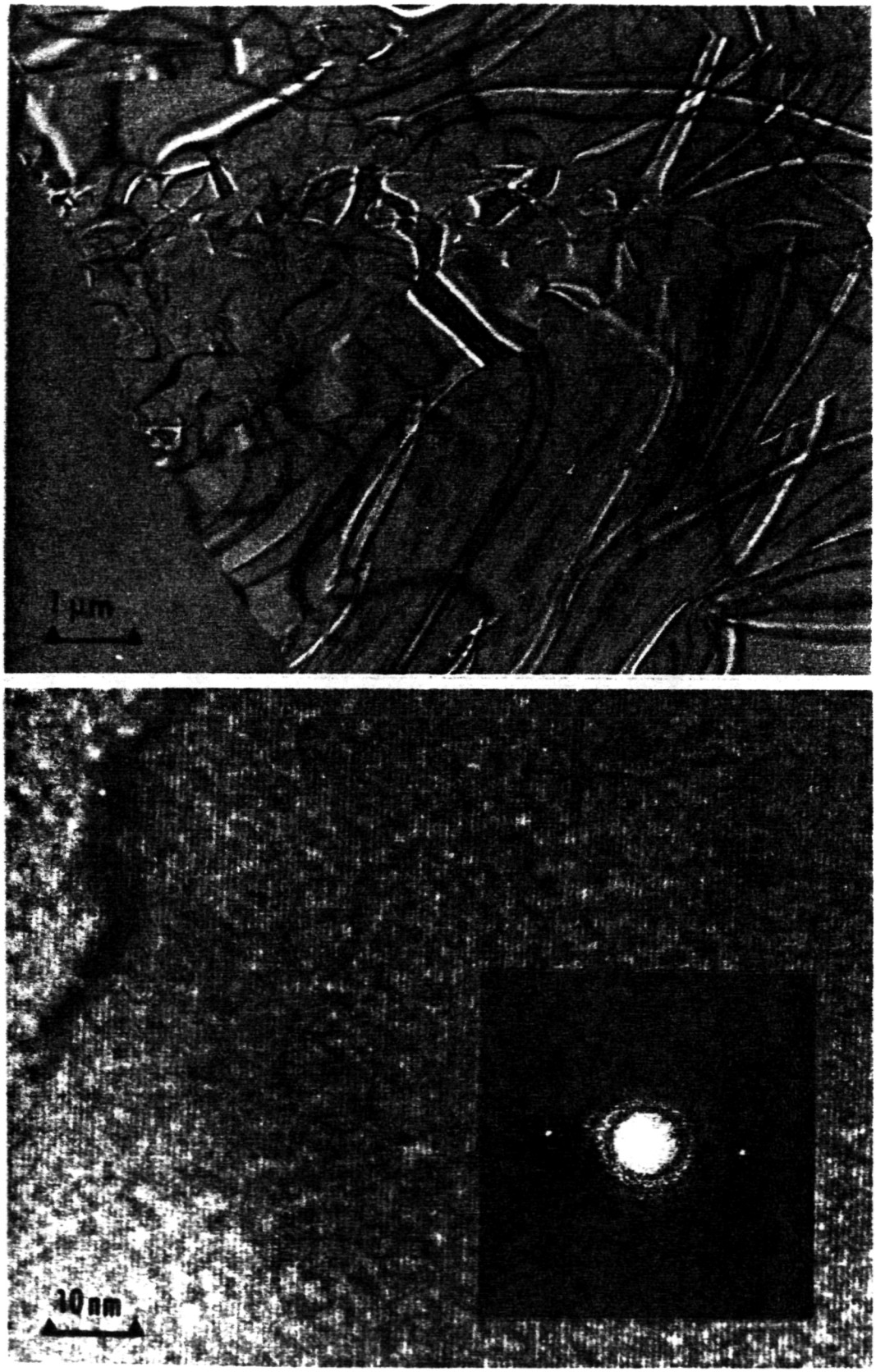

Fig. 10

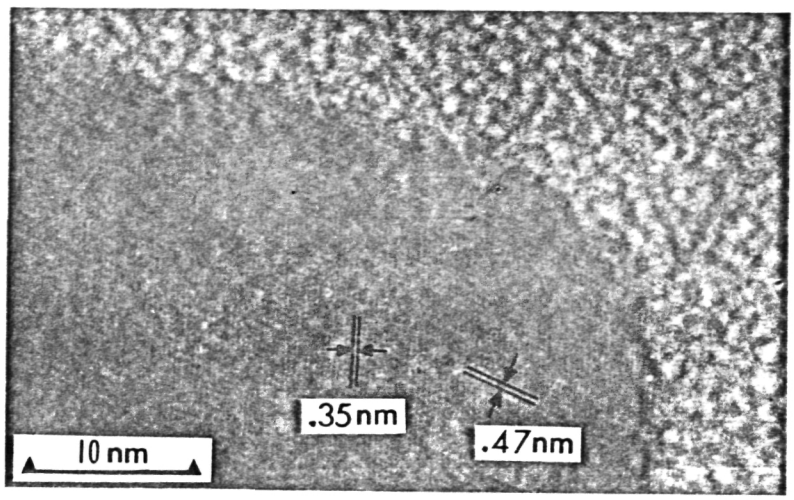

Fig. 11

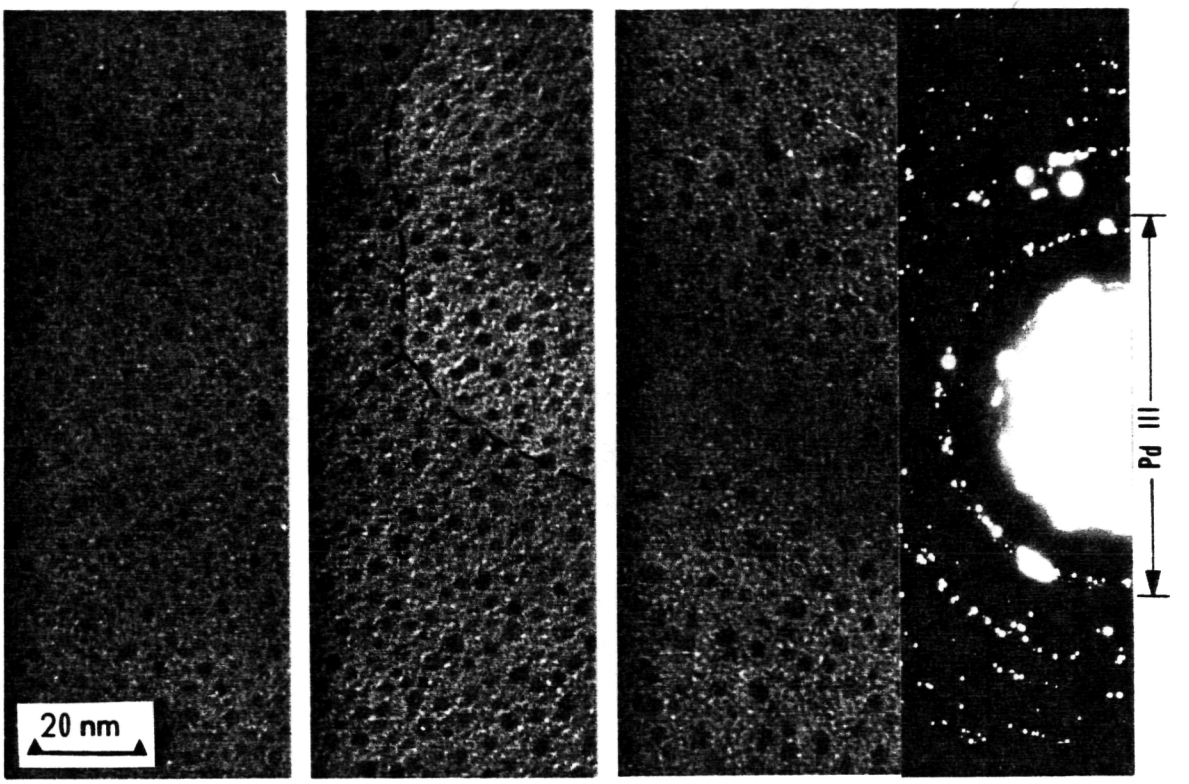

Fig. 12

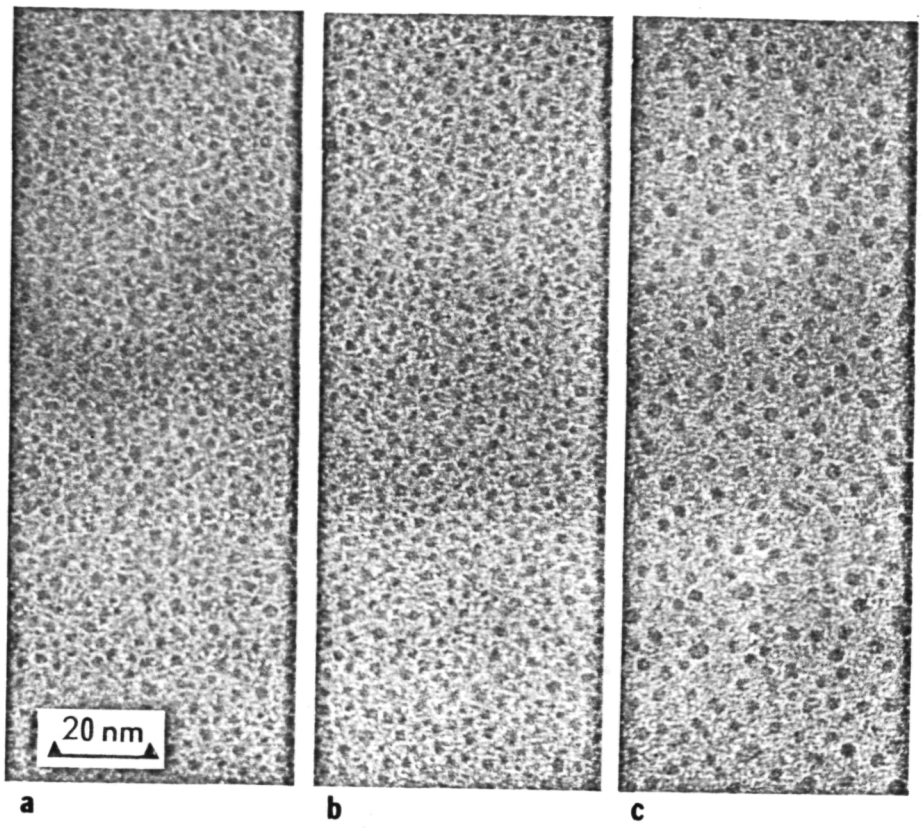

Fig. 13

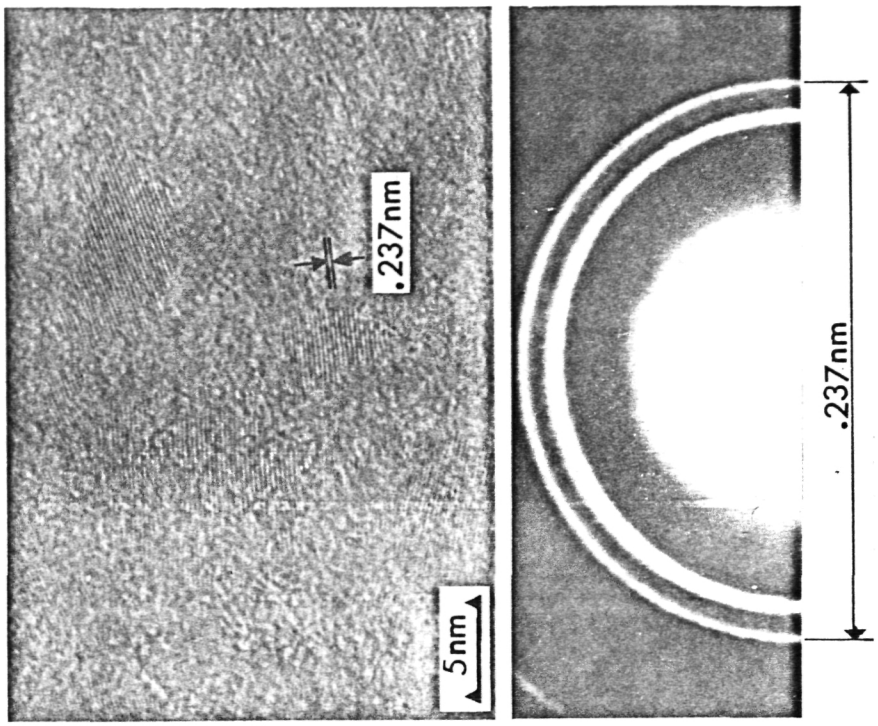

Fig. 14

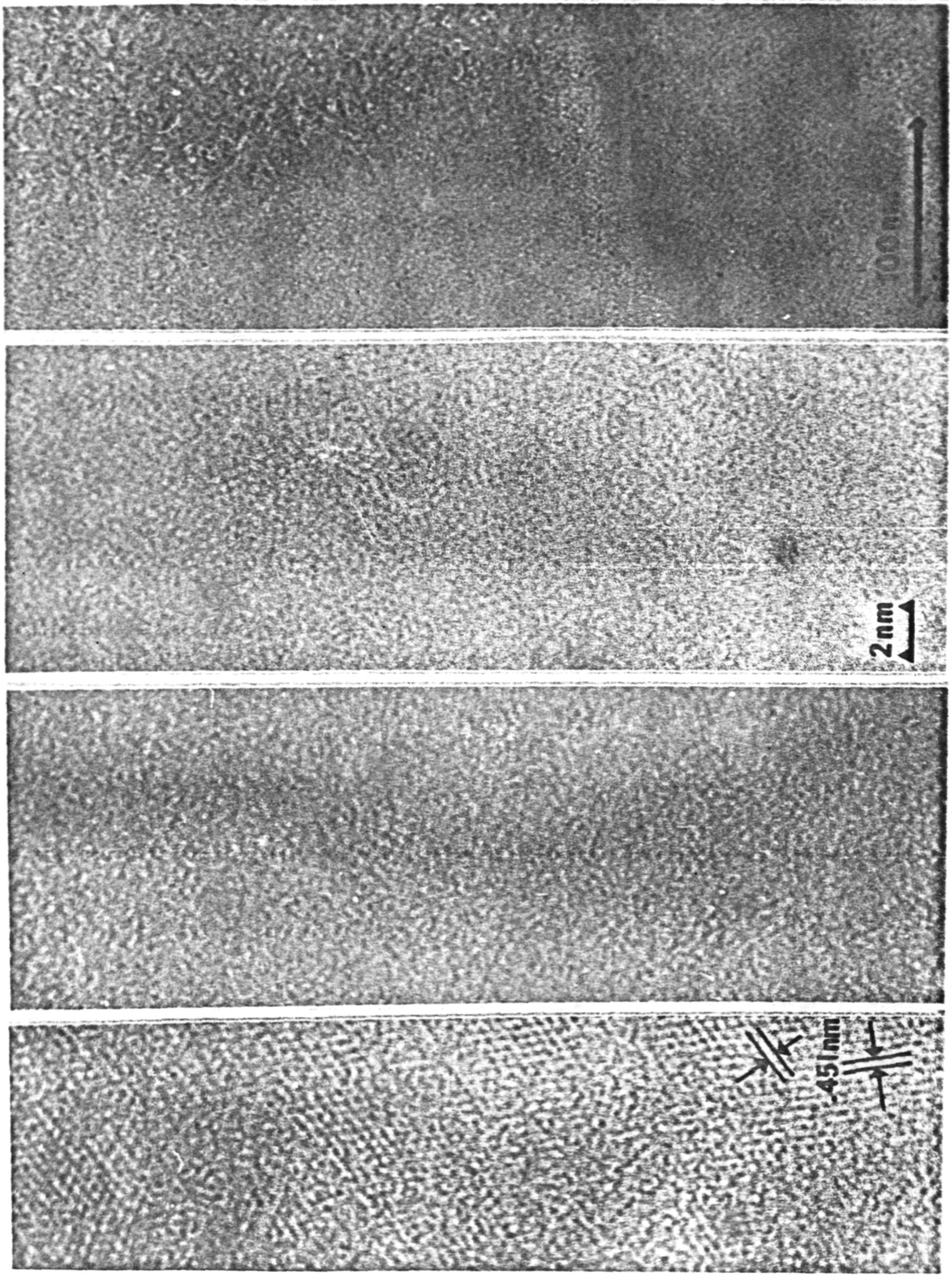

Fig. 15